Inorganic Chemistry

Article

pubs.acs.org/IC

Ferro- to Antiferromagnetic Crossover Angle in Diphenoxido- and Carboxylato-Bridged Trinuclear Ni^{II}_2–Mn^{II} Complexes: Experimental Observations and Theoretical Rationalization

Piya Seth,[†] Albert Figuerola,*[,‡,§] Jesús Jover,[‡,∥] Eliseo Ruiz,[‡,∥] and Ashutosh Ghosh*[,†]

[†]Department of Chemistry, University College of Science, University of Calcutta, 92, A.P.C. Road, Kolkata 700 009, India

[‡]Departament de Química Inorgànica, Universitat de Barcelona, Martí i Franquès 1-11, 08028 Barcelona, Spain

[§]Institut de Nanociència i Nanotecnologia (IN2UB), Universitat de Barcelona, Martí i Franquès 1-11, 08028 Barcelona, Spain

[∥]Institut de Recerca de Química Teòrica i Computacional, Universitat de Barcelona, Diagonal 645, E-08028 Barcelona, Spain

Supporting Information

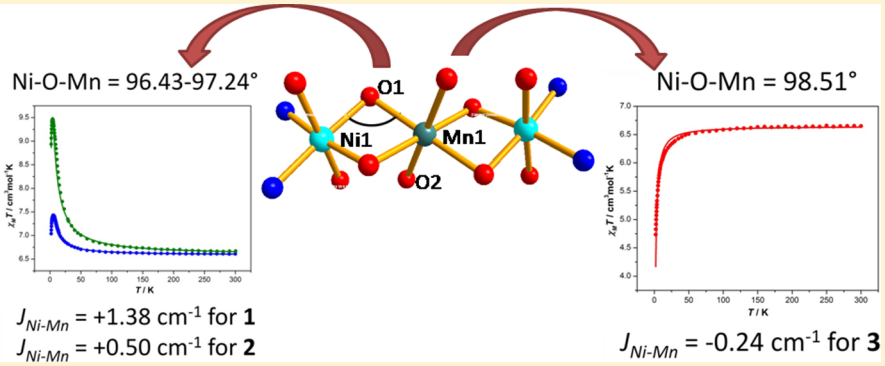

ABSTRACT: Three new trinuclear heterometallic Ni^{II}–Mn^{II} complexes have been synthesized using a [NiL] metalloligand, where H_2L = *N,N′*-bis(salicylidene)-1,3-propanediamine. The complexes $[(NiL)_2Mn(OCnn)_2(CH_3OH)_2]\cdot CH_3OH$ (**1**), $[(NiL)_2Mn(OPh)_2(CH_3OH)_2][(NiL)_2Mn(OPh)_2]\cdot H_2O$ (**2**), and $[(NiL)_2Mn(OSal)_2(CH_3OH)_2]\cdot 2[NiL]$ (**3**) (where OCnn = cinnamate, OPh = phenylacetate, OSal = salicylate) have been structurally characterized. In all three complexes, in addition to the double phenoxido bridge, the two terminal Ni^{II} atoms are linked to the central Mn^{II} by means of a *syn-syn* bridging carboxylate, giving rise to a linear structure. Complexes **1** and **2** with Ni–O–Mn angles of 97.24 and 96.43°, respectively, exhibit ferromagnetic interactions (J_{Ni-Mn} = +1.38 and +0.50 cm^{-1}, respectively), whereas **3** is antiferromagnetic (J_{Ni-Mn} = −0.24 cm^{-1}), having an Ni–O–Mn angle of 98.51°. DFT calculations indicate that there is a clear magneto-structural correlation between the Ni–O–Mn angle and J_{Ni-Mn} values, which is in agreement with the experimental results.

INTRODUCTION

The rational design and synthesis of oxido- or phenoxido-bridged molecular assemblies formed by a finite number of exchange-coupled paramagnetic centers have attracted the attention of inorganic chemists for a long time. The majority of the species that have been studied are homometallic. Among them, homonuclear Cu^{II},[1] Ni^{II},[2] and Mn^{III} [3] complexes derived from di-Schiff base ligands and various bridging coligands are of considerable interest because of their fascinating structural features and intriguing magnetic properties. These compounds also play a key role in deriving the magneto-structural correlations for oxido- and/or phenoxido-bridged metal complexes. From the experimental and theoretical results, it can be said that the magnetic exchange interactions in this class of compounds depend on several factors: e.g. M–O–M angle, M–O distance, the effect of the asymmetry on the metal–bridge bonds, and the hinge distortion of the M_2O_2 core.[4] Detailed DFT calculations showing the dependence of the coupling constant J on the phenoxido bridging angle in homometallic dinuclear Cu^{II}, Ni^{II}, and Mn^{III} complexes have been performed to quantify the respective contributions of ferro-/antiferromagnetic interactions. From both theoretical calculations and experimental results, it has been found that for dinuclear Cu^{II} complexes ferromagnetism appears for a bridging Cu–O–Cu angle lower than 92.4°.[1a] The critical phenoxido bridging angle is 93.5° for μ_2-O-bridged dinuclear Ni^{II} complexes[2a] and 101° for Mn^{III} complexes.[3d,e]

The number of oxido-/phenoxido-bridged heterometallic Cu^{II}, Ni^{II}, and Mn^{III} complexes of salen type Schiff base ligands is relatively less than that of the corresponding homometallic complexes. Moreover, in most of these complexes the metal ions are Cu^{II}–Ni^{II} [5] and Cu^{II}–Mn^{II}.[6] The number of Ni^{II}–Mn^{II} complexes with this type of ligand is relatively scanty, and very

Received: June 17, 2014
Published: August 11, 2014

   dx.doi.org/10.1021/ic501425x | *Inorg. Chem.* 2014, 53, 9296–9305

few of them have been magnetically characterized. A recently updated CSD search reveals that the number of diphenoxido-bridged Ni^{II}–Mn^{II} complexes with salen type Schiff base ligands is 11,[7−9] among which only 2 have been magnetically characterized.[7,8] Between these two complexes, one having an Ni–O–Mn angle of 86.38° is ferromagnetically coupled (J_{Ni-Mn} = +9.3 cm^{-1}) while the other shows antiferromagnetic interactions (J_{Ni-Mn} = −0.30 cm^{-1}) with an Ni–O–Mn angle of 102.31°. The results clearly suggest that a critical angle should exist in between, and therefore it is worth to designing and synthesizing some Ni^{II}–Mn^{II} heterometallic complexes with the phenoxido bridging angle within the range 86–102°, so that one can have an idea of the critical angle for this system. An efficient strategy for synthesizing heterometallic complexes of salen type Schiff base ligands is to employ the "metalloligand" approach. The use of various bridging and/or terminally coordinating anionic coligands plays an important role in controlling the phenoxido bridging angle and consequently the magnetic coupling.[10] Recently, we reported some trinuclear Cu^{II}–Mn^{II} complexes using the [CuL] metalloligand (where H_2L= *N*,*N*′-bis(salicylidene)-1,3-propanediamine). Although the Cu–O–Mn bridging angles in these complexes have been varied in a wide range of 92–101° by suitably selecting the anionic coligands, the antiferro- to ferromagnetic crossover angle was not detected.[6e] However, for Ni^{II}–Mn^{II} complexes the experimental search for critical angle should end in success by narrowing down the range, as both ferromagnetically and antiferromagnetically coupled complexes are known.[7,8] The aim of the present investigation is therefore to synthesize some Ni^{II}–Mn^{II} complexes with the variation of phenoxido bridging angles and to study their magnetic properties. We also want to substantiate the experimental magnetic coupling with the help of DFT studies, which have rarely been done for such heterometallic compounds.

Herein we report the synthesis, crystal structure, and magnetic properties of the three new complexes $[(NiL)_2Mn(OCnn)_2(CH_3OH)_2]\cdot CH_3OH$ (**1**), $[(NiL)_2Mn(OPh)_2(CH_3OH)_2][(NiL)_2Mn(OPh)_2]\cdot H_2O$ (**2**), and $[(NiL)_2Mn(OSal)_2(CH_3OH)_2]\cdot 2[NiL]$ (**3**), where OCnn = cinnamate, OPh = phenylacetate, and OSal = salicylate. Among these, complexes **1** and **2** have average Ni–O–Mn angles of 97.24 and 96.43°, respectively, exhibiting ferromagnetic interactions with J_{Ni-Mn} values of +1.38 and +0.50 cm^{-1}. For **3** the Ni–O–Mn angle is 98.51°, corresponding to antiferromagnetic interactions (J_{Ni-Mn} = −0.24 cm^{-1}). For the title heterometallic complexes theoretical calculations support the experimentally observed fact that the Ni^{II}–Mn^{II} systems have a large tendency to show ferromagnetic coupling because of predominating orthogonally oriented magnetic orbitals of the two metal ions, and larger Ni–O–Mn angles (above 98°) are responsible for antiferromagnetic spin exchange.

EXPERIMENTAL SECTION

Synthesis of Manganese Carboxylates. The three metal carboxylate salts, viz. $Mn(OCnn)_2$ $Mn(OPh)_2\cdot H_2O$, and $Mn(OSal)_2$, were prepared by following similar procedures. To an aqueous solution (30 mL) of the corresponding carboxylic acid (148.16 mg of cinnamic acid, 136.15 mg of phenylacetic acid, or 138.12 mg of salicylic acid) was added manganese carbonate (60.0 mg) in small portions with constant stirring with a glass rod until effervescence ceased. Then the mixture was warmed on a water bath for 10–15 min and filtered. The clear filtrate was kept over a water bath until a solid started to separate. The solution was then cooled to room temperature, and the crystalline solid product was filtered through suction and dried under vacuum. All other chemicals are of commercial reagent grade and were used as received, without further purification.

Synthesis of the Schiff-Base Ligand *N*,*N*′-Bis(salicylidene)-1,3-propanediamine (H_2L). The di-Schiff base ligand H_2L was synthesized in our laboratory by standard methods.[11] Salicylaldehyde (1.05 mL, 10 mmol) was mixed with 1,3-propanediamine (0.42 mL, 5 mmol) in methanol (20 mL). The resulting mixture was refluxed for ca. 1.5 h and cooled. The desired yellow crystalline ligand was filtered off, washed with methanol, and dried in a vacuum desiccator containing anhydrous $CaCl_2$.

Preparation of the "Metalloligand" [NiL]. A mixture of H_2L (1.432 g, 5 mmol) in methanol and ammonia solution (10 mL, 20%) was added to a methanolic solution (20 mL) of $Ni(ClO_4)_2\cdot 6H_2O$ (1.825 g, 5 mmol) to prepare the "ligand complex" [NiL] as previously reported.[12]

Synthesis of Complexes 1–3. To a 20 mL methanolic solution of [NiL] (0.321 g, 1 mmol) were added an aqueous solution (5 mL) of $Mn(OCnn)_2$ (0.175 g, 0.5 mmol), $Mn(OPh)_2\cdot H_2O$ (0.172 g, 0.5 mmol) and $Mn(OSal)_2$ (0.165 g, 0.5 mmol) for **1**–**3**, respectively, and the mixtures were stirred for ca. 1 h at room temperature. A green precipitate that separated from the reaction mixture in each case was filtered and the respective filtrates were allowed to stand overnight. Deep green X-ray-quality single crystals appeared on the wall of the vessel on slow evaporation of the solvent in each case. The crystals were isolated, washed with methanol, and dried in a desiccator containing anhydrous $CaCl_2$.

Complex ***1***. Yield: 0.410 g (71%) Anal. Calcd for $C_{56}H_{61}N_4O_{12}Ni_2Mn$ (1154.41): C, 58.26; H, 5.33; N, 4.85. Found: C, 58.12; H, 5.29; N, 4.73. IR (KBr pellet, cm^{-1}): 1638 ν(C=N), 1578 ν_{as}(COO), 1468 ν_s(COO). λ_{max} (MeOH, nm): 350, 409 599.

Complex ***2***. Yield: 0.388 g (74%). Anal. Calcd for $C_{51}H_{50}N_4O_{10}Ni_2Mn$ (1051.26): C, 58.27; H, 4.79; N, 5.33. Found: C, 58.18; H, 4.70; N, 5.26. IR (KBr pellet, cm^{-1}): 1635 ν(C=N), 1588 ν_{as}(COO), 1469 ν_s(COO). λ_{max} (MeOH, nm): 356, 407, 592.

Complex ***3***. Yield: 0.297 g (68%). Anal. Calcd for $C_{84}H_{82}N_8O_{16}Ni_4Mn$ (1749.28): calcd C, 57.67; H, 4.72; N, 6.41. Found: C, 57.56; H, 4.65; N, 6.35. IR (KBr pellet, cm^{-1}): 1625 ν(C=N), 1541 ν_{as}(COO), 1463 ν_s(COO). λ_{max} (MeOH, nm): 349, 408, 597.

Physical Measurements. Elemental analyses (C, H, and N) were performed using a PerkinElmer 240C elemental analyzer. IR spectra in KBr (4000–500 cm^{-1}) were recorded using a PerkinElmer RXI FTIR spectrophotometer. Temperature-dependent molar susceptibility measurements of powdered polycrystalline samples of **1**–**3** were carried out at the "Servei de Magnetoquímica (Universitat de Barcelona)" in a Quantum Design SQUID MPMSXL susceptometer with applied fields of 3000 and 198 G in the temperature ranges 2–300 and 2–30 K, respectively.

Computational Details. To calculate the exchange interactions, a phenomenological Heisenberg–Dirac–van Vleck Hamiltonian was used, excluding the terms relating to magnetic anisotropy, to describe the exchange coupling in a general polynuclear complex:

$$\hat{H} = -\sum_{a<b} J_{ab}\hat{S}_a\hat{S}_b \qquad (1)$$

where $\hat{S}_a$ and $\hat{S}_b$ are the spin operators of the different paramagnetic cations. The J_{ab} parameters are the pairwise coupling constants between the paramagnetic centers of the molecule. Basically, we need to calculate the energy of n + 1 spin distributions for a system with n different exchange coupling constants.[13−17] These energy values allow us to build up a system of n equations in which the J values are the unknowns. In the present study, three calculations were performed in order to obtain the two exchange coupling constants of the $MnNi_2$ complexes. They correspond to the high-spin S = 9/2 state, one S = 1/2 wave function flipping the spin of the central manganese atom, and finally one S = 5/2 state with the spin inversion of the two external nickel atoms. Theoretical calculations were performed with the hybrid B3LYP functional[18] as implemented in Gaussian09 code[19] using a guess function generated with the Jaguar 7.0 code,[20] which employs a procedure that allows us to determine individually the local charges and multiplicities of the atoms, including the ligand field effects.[21] A triple-ζ all-electron Gaussian basis set was used for all atoms.[22]

dx.doi.org/10.1021/ic501425x | *Inorg. Chem.* 2014, 53, 9296–9305

Table 1. Crystal Data and Structure Refinement of Complexes 1−3

	1	2	3
formula	$C_{56}H_{61}N_4O_{12}Ni_2Mn$	$C_{51}H_{50}N_4O_{10}Ni_2Mn$	$C_{84}H_{82}N_8O_{16}Ni_4Mn$
formula wt	1154.41	1051.26	1749.28
space group	$P\bar{1}$	$P\bar{1}$	$P\bar{1}$
cryst syst	triclinic	triclinic	triclinic
a/Å	10.8407(9)	9.3692(13)	12.004(5)
b/Å	14.1770(12)	10.5173(14)	12.166(5)
c/Å	18.5894(16)	23.878(3)	14.238(5)
α/deg	90.611(4)	90.311(2)	89.107(5)
β/deg	92.259(4)	99.130(2)	69.512(5)
γ/deg	104.275(3)	90.807(2)	88.037(5)
V/Å^3	2766.0(4)	2322.8(5)	1946.6(13)
Z	2	2	1
calcd density D_{calcd}/g cm^{-3}	1.386	1.503	1.492
abs coeff (μ)/mm^{-1}	0.962 (Mo Kα)	1.135 (Mo Kα)	1.181 (Mo Kα)
F(000)	1204.0	1090.0	907
R(int)	0.030	0.021	0.025
θ range/deg	1.1−28.4	0.9−26.4	1.5−26.5
total no. of rflns	35517	17569	24251
no. of unique rflns	13444	8940	7783
no. of rflns with $I > 2\sigma(I)$	10683	7044	6454
R1, wR2	0.0438, 0.1341	0.0413, 0.1104	0.0358, 0.1031
temp/K	293	293	293

Crystal Data Collection and Refinement. Suitable single crystals of complexes **1**−**3** were mounted on a Bruker-AXS SMART APEX II diffractometer equipped with a graphite monochromator and Mo Kα (λ = 0.71073 Å) radiation. The crystals were positioned at 60 mm from the CCD. A total of 360 frames were measured with a counting time of 10 s. The structures were solved by the Patterson method using SHELXS 97. Subsequent difference Fourier synthesis and least-squares refinement revealed the positions of the remaining non-hydrogen atoms, which were refined with independent anisotropic displacement parameters. Hydrogen atoms were placed in idealized positions, and their displacement parameters were fixed to be 1.2 times larger than those of the attached non-hydrogen atom. Absorption corrections were carried out using the SADABS program.[23] All calculations were carried out using SHELXS 97,[24] SHELXL 97,[25] PLATON 99,[26] ORTEP-32,[27] and WinGX system Ver-1.64.[28] Data collection and structure refinement parameters and crystallographic data for the three complexes are given in Table 1.

RESULTS AND DISCUSSION

Syntheses and IR and Electronic Spectra of the Complexes. Three new Ni^{II}−Mn^{II} carboxylate complexes derived from the Schiff base H_2L were synthesized by following similar procedures. For this purpose, we first prepared the metalloligand [NiL] by a reported procedure.[12] An aqueous solution of the respective manganese carboxylate was then mixed with a methanolic solution of this metalloligand [NiL] to give the desired complexes (Scheme 1). In addition to elemental analysis, all three complexes were characterized by IR spectroscopy. For **1**−**3** a strong and sharp band appeared at 1638, 1635, and 1625 cm^{-1}, respectively, due to azomethine ν(C═N). Other peaks due to asymmetric and symmetric stretching of the carboxylate are observed at 1578, 1468 cm^{-1} (in **1**) 1588, 1469 cm^{-1} (in **2**), and 1541, 1463 cm^{-1} (in **3**), respectively. Electronic spectra of the three complexes in methanol solvent are similar, having two strong peaks at 350, 409 nm (in **1**), 356, 407 nm (in **2**), and 349, 408 nm (in **3**), which correspond to ligand to metal charge transfer transitions. Another strong absorption band is observed at 599, 592, and 597 nm for **1**−**3**, respectively, which can be assigned to the d−d transitions in Ni^{II} complexes.

Scheme 1. Formation of Complexes 1−3

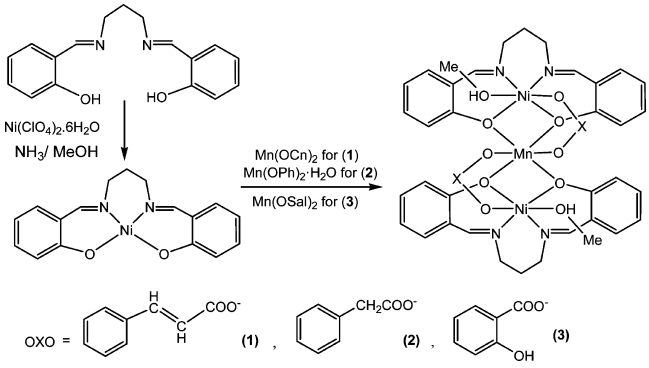

Description of Structures. The X-ray crystal structure of **1** reveals that it consists of two similar centrosymmetric trinuclear units **1A**,**B** having the same composition [(NiL)$_2$Mn(OCnn)$_2$(CH$_3$OH)$_2$]·CH$_3$OH. An ORTEP diagram of **1A** is shown in Figure 1. Here, both the units contain a six-coordinate Mn^{II} in a distorted-octahedral environment together with two six-coordinated octahedral Ni^{II} atoms having equivalent geometries. The manganese atom is situated at the center of inversion and is bonded to four oxygen atoms from the two ligands L, which form the basal plane of the Mn^{II}, while the trans axial positions are occupied by the oxygen atom O(4) (in **1A**) and O(8) (in **1B**) of the *syn-syn* bridging cinnamate (bond distances are given in Table 2).

The two terminal nickel atoms are bonded to four donor atoms (O(1), O(2), N(1), N(2) in **1A** and O(6), O(7), N(3), N(4) in **1B**) of the ligand L, making up the equatorial plane. One of the axial positions is occupied by an oxygen atom (O(3) in **1A**, O(9) in **1B**) of the *syn-syn* bridging cinnamate. The other axial positions of the nickel atoms are bonded to the oxygen atom of the solvent methanol. The mean deviation of

dx.doi.org/10.1021/ic501425x | Inorg. Chem. 2014, 53, 9296−9305

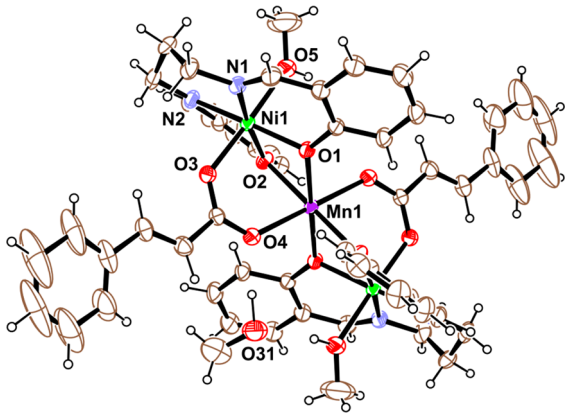

Figure 1. ORTEP-3 view of the centrosymmetric trinuclear structure of **1A** with ellipsoids at the 30% probability level. There are two trimers with equivalent structures; only one is shown.

four donor atoms in the basal plane from their respective mean plane are 0.003 Å (in **1A**) and 0.031 Å (in **1B**), while the Ni atom deviates by 0.024(1) Å in the direction of the axial O(3) in **1A** and 0.004(1) Å toward O(9) in **1B**. The Ni···Mn distance is 3.149(4) Å in **1A** and 3.133(4) Å in **1B**. The two Ni−O−Mn bridging angles are 97.29(7), 97.74(7)° in **1A** and 95.52(7), 98.36(8)° in **1B**.

Complex **2** also consists of two centrosymmetric trinuclear units $[(NiL)_2Mn(OPh)_2(CH_3OH)_2]\cdot H_2O$ (**2A**) and $[(NiL)_2Mn(OPh)_2]$ (**2B**), but the compositions of the units are different. An ORTEP diagram of **2A** is shown in Figure 2. Each of the two units contains two terminal Ni^{II} atoms and a central Mn^{II}. Each unit contains a six-coordinated manganese in a distorted-octahedral environment at the center of inversion that is bonded to four oxygens from the two ligands L, which form the basal plane of the Mn^{II}. The trans axial positions are occupied by the oxygen atom O(4) (in **2A**) and O(8) (in **2B**) of the *syn-syn* bridging phenylacetate (bond distances are given in Table 2).

The two terminal nickel atoms are bonded to four donor atoms (O(1), O(2), N(1), N(2) in **2A** and O(6), O(7), N(3), N(4) in **2B**) of the tetradentate ligand L, making up the equatorial plane. The fifth coordination site is occupied by a bridging oxygen atom (O(3) in **2A**, O(9) in **2B**) of the *syn-syn* bridging phenylacetate. The other axial position of the nickel atoms in **2A** is bonded to the oxygen atom of the solvent methanol, whereas this second axial position is vacant in **2B**. Thus, the Ni atoms are hexacoordinated with a distorted-octahedral environment in **2A**, whereas these atoms are pentacoordinated in **2B** with a geometry closer to square pyramidal, as indicated by the Addison parameter (τ = 0.067). τ = 0 for an ideal square pyramid and τ = 1 for a trigonal bipyramid.[29] The mean deviations of four donor atoms in the basal plane from their respective mean plane are 0.005 and 0.042 Å in **2A**,**B**, respectively. The Ni atom deviates by 0.040(1) Å in the direction of the axial O(3) in **2A** and −0.271(1) Å in the direction of the axial O(9) in **2B**. The Ni···Mn distance is 3.135(6) Å in **2A** and 3.091(5) Å in **2B**. Two Ni−O−Mn bridging angles are 96.58(8), 97.34(8)° in **2A** and 95.83(8), 95.87(7)° in **2B**.

The X-ray crystal structure analysis shows that **3** contains two units, namely $[(NiL)_2Mn(OSal)_2(CH_3OH)_2]$ (**3A**) and [NiL] (**3B**). Of these, **3A** has a trinuclear centrosymmetric structure containing two terminal Ni^{II} atoms and a central Mn^{II} (Figure 3). The octahedral manganese atom is bonded to four oxygen atoms from the two ligands L, which form the basal plane of the Mn^{II}, while the trans axial positions are occupied by the oxygen atom O(4) of the *syn-syn* bridging salicylate. The two terminal nickel atoms are bonded to four donor atoms (O(1), O(2), N(1), and N(2)) of the ligand L, making up the equatorial plane. One of the axial positions is occupied by the bridging oxygen atom O(3) of the *syn-syn* bridging salicylate. The other axial positions of the nickel atoms are also bonded to the oxygen atom of the solvent methanol that completes a distorted-octahedral environment around the Ni atom. The mean deviation of four donor atoms in the basal plane from their respective mean plane is 0.030 Å, while the Ni atom deviates by 0.008(1) Å in the direction of the axial O(3). The Ni···Mn distance is 3.171(1) Å, and the two Ni−O−Mn bridging angles are 98.31(7) and 98.70(7)° (Table 2).

3B consists of a mononuclear [NiL] unit where four-coordinated square-planar nickel is bonded to the donor atoms O(6), O(7), N(3), N(4) of L (Figure 4). The Ni−O and Ni−N distances (Table 2) are shorter than the corresponding distances in **1A**,**B**, **2A**,**B**, and **3A**, which is quite usual for a square-planar geometry.[30] The τ_4 value for Ni(2) is 0.154, which indicates a slightly distorted square-planar geometry around it.[31]

In this context it is to comparing the structural features of similar kinds of reported diphenoxido- and carboxylato-bridged linear trinuclear Ni^{II}_2−Mn^{II} complexes derived from N_2O_2 donor di-Schiff base ligands. There are three such complexes in which the phenoxido bridging angle varies in the range 94−96°.[9a,b,d] When the carboxylato groups were replaced by pseudohalides, bent trinuclear Ni^{II}_2−Mn^{II} complexes resulted with a wider phenoxido bridging angle in the range 100−103°.[30a] On the other hand, there is only one carboxylato-bridged Ni^{II}_2−Mn^{II} complex of a tridentate N_2O donor Schiff base ligand, and the Ni−O−Mn angle in that compound is ∼102°.[7] Another complex based on ha exadentate N_3O_3 donor Schiff base ligand has been reported with an Ni−O−Mn angle of ∼86°.[8] It should be mentioned here that, in the present complexes, the phenoxido bridging angle varies from 96.43 to 98.51°.

Magnetic Properties. Magnetic measurements in complexes **1** and **2** show clear ferromagnetic interactions between Ni^{II} and Mn^{II} ions within the complexes, while antiferromagnetic exchange becomes obvious in complex **3**. Temperature-dependent molar susceptibility measurements on polycrystalline samples of **1**−**3** were carried out in an applied field of 0.3 T in the temperature range 1.9−300 K. The data are shown in the $\chi_M T$ versus T plot in Figure 5, where χ_M is the molar magnetic susceptibility and T is the absolute temperature. The room-temperature values of $\chi_M T$ for compounds **1**−**3** are 6.67, 6.61, and 6.63 $cm^3\ mol^{-1}$ K, respectively, slightly higher than the 6.4 $cm^3\ mol^{-1}$ K value expected for noninteracting Ni^{II}−Mn^{II}−Ni^{II} trinuclear units. For complexes **1** and **2**, the $\chi_M T$ values increase with decreasing temperature until they reach a maximum of 9.47 $cm^3\ mol^{-1}$ K at 4.5 K for **1** and 7.43 $cm^3\ mol^{-1}$ K at 6 K for **2**. Below these temperatures, the value of $\chi_M T$ drops sharply. On the other hand, the $\chi_M T$ values measured for complex **3** remain approximately constant down to 50 K; below that temperature, they suddenly drop. In order to quantitatively interpret these data, simulations of the experimental curves were carried out by using the MAGPACK program as shown in Figure 5.[32] A Hamiltonian of the type $H = -J[S_1S_2 + S_1S_3]$, where $S_1 = S_{Mn}$ and $S_2 = S_3 = S_{Ni}$, was used for

dx.doi.org/10.1021/ic501425x | Inorg. Chem. 2014, 53, 9296−9305

Table 2. Dimensions in the Metal Coordination Spheres in 1A,B, 2A,B, and 3A,B (Distances in Å, Angles in deg)

	1A	2A	3A		1B	2B	3B
Ni(1)−O(1)	2.028(2)	2.016(2)	2.016(2)	Ni(2)−O(6)	2.017(2)	2.002(2)	1.845(3)
Ni(1)−O(2)	2.023(2)	2.022(2)	2.006(2)	Ni(2)−O(7)	2.020(2)	1.999(2)	1.862(2)
Ni(1)−O(3)	2.055(2)	2.054(3)	2.095(2)	Ni(2)−N(3)	2.030(2)	2.017(2)	1.889(3)
Ni(1)−O(5)	2.153(2)	2.153(3)	2.185(2)	Ni(2)−N(4)	2.022(2)	2.014(2)	1.900(5)
Ni(1)−N(1)	2.024(2)	2.021(3)	2.037(2)	Ni(2)−O(9)	2.052(2)	1.995(2)	
Ni(1)−N(2)	2.035(2)	2.016(3)	2.042(2)	Ni(2)−O(10)	2.147(3)		
Mn(1)−O(2)	2.170(2)	2.175(2)	2.171(2)	Mn(2)−O(6)	2.212(2)	2.161(2)	
Mn(1)−O(4)	2.210(2)	2.199(2)	2.185(2)	Mn(2)−O(6)^b	2.212(2)	2.161(2)	
Mn(1)−O(1)	2.158(2)	2.158(2)	2.174(2)	Mn(2)−O(7)	2.120(2)	2.163(2)	
Mn(1)−O(4)^a	2.210(2)	2.199(2)	2.185(2)	Mn(2)−O(7)^b	2.120(2)	2.163(2)	
Mn(1)−O(1)^a	2.151(2)	2.158(2)	2.174(2)	Mn(2)−O(8)	2.225(2)	2.138(2)	
Mn(1)−O(2)^a	2.170(2)	2.175(2)	2.171(2)	Mn(2)−O(8)^b	2.225(2)	2.138(2)	
O(1)−Ni(1)−O(2)	82.31(7)	83.30(8)	80.04(6)	N(3)−Ni(2)−N(4)	97.25(9)	95.50(9)	94.16(14)
O(1)−Ni(1)−O(3)	92.50(7)	91.61(8)	91.40(7)	O(7)−Ni(2)−N(4)	89.76(9)	89.68(8)	92.36(12)
O(1)−Ni(1)−O(5)	88.99(8)	87.55(10)	91.51(7)	O(7)−Ni(2)−N(3)	172.74(8)	165.00(8)	168.91(11)
O(1)−Ni(1)−N(1)	90.59(8)	90.70(11)	90.78(7)	O(6)−Ni(2)−O(7)	82.14(7)	81.91(8)	80.89(10)
O(1)−Ni(1)−N(2)	173.18(8)	172.45(11)	170.18(8)	O(6)−Ni(2)−N(3)	90.91(8)	88.84(8)	93.86(13)
O(2)−Ni(1)−O(3)	94.05(7)	95.22(9)	95.05(7)	O(6)−Ni(2)−N(4)	171.72(8)	160.97(8)	169.27(13)
O(2)−Ni(1)−O(5)	88.07(10)	89.63(9)	89.53(8)	O(7)−Ni(2)−O(9)	94.77(8)	100.08(8)	
O(2)−Ni(1)−N(1)	172.82(8)	173.73(11)	170.70(7)	O(9)−Ni(2)−N(3)	87.64(8)	93.28(8)	
O(2)−Ni(1)−N(2)	91.03(8)	89.58(11)	90.42(8)	O(9)−Ni(2)−N(4)	86.08(9)	96.92(9)	
O(3)−Ni(1)−O(5)	177.56(10)	174.95(10)	174.94(8)	O(6)−Ni(2)−O(9)	92.90(7)	101.33(8)	
O(3)−Ni(1)−N(1)	87.28(8)	86.75(13)	86.59(8)	O(6)−Ni(2)−O(10)	89.53(10)		
O(3)−Ni(1)−N(2)	89.44(8)	91.52(10)	87.13(7)	O(7)−Ni(2)−O(10)	89.01(9)		
O(5)−Ni(1)−N(1)	90.77(11)	88.29(13)	89.23(9)	O(9)−Ni(2)−O(10)	175.75(9)		
O(5)−Ni(1)−N(2)	89.30(9)	89.93(12)	90.70(8)	O(10)−Ni(2)−N(3)	88.84(10)		
N(1)−Ni(1)−N(2)	96.04(9)	96.33(13)	98.82(9)	O(10)−Ni(2)−N(4)	92.01(11)		
O(2)−Mn(1)−O(4)^a	92.15(7)	92.77(7)	90.04(6)	O(7)−Mn(2)−O(7)^b	180.00	180.00	
O(4)−Mn(1)−O(4)^a	180.00	180.00	180.00	O(6)−Mn(2)−O(7)	75.48(7)	74.65(7)	
O(1)^a−Mn(1)−O(2)^a	76.19(6)	76.53(7)	73.08(6)	O(6)−Mn(2)−O(8)	91.84(7)	86.74(7)	
O(1)^a−Mn(1)−O(4)^a	86.29(7)	85.62(7)	90.73(7)	O(6)−Mn(2)−O(6)^b	180.00	180.00	
O(2)^a−Mn(1)−O(4)^a	87.85(7)	87.23(7)	89.97(6)	O(6)−Mn(2)−O(7)^b	104.52(7)	105.35(7)	
O(1)−Mn(1)−O(4)^a	93.71(7)	94.38(7)	89.27(7)	O(6)−Mn(2)−O(8)^b	88.16(7)	93.26(7)	
O(1)^a−Mn(1)−O(4)	93.71(7)	94.38(7)	89.27(7)	O(7)−Mn(2)−O(8)^b	93.66(7)	93.37(7)	
O(2)^a−Mn(1)−O(4)	92.15(7)	92.77(7)	90.04(6)	O(6)^b−Mn(2)−O(8)	88.16(7)	93.26(7)	
O(1)−Mn(1)−O(2)	76.19(6)	76.53(7)	73.08(6)	O(7)^b−Mn(2)−O(8)	93.66(7)	93.37(7)	
O(1)−Mn(1)−O(4)	86.29(7)	85.62(7)	90.73(7)	O(8)−Mn(2)−O(8)^b	180.00	180.00	
O(1)−Mn(1)−O(1)^a	180.00	180.00	180.00	O(6)^b−Mn(2)−O(7)^b	75.48(7)	74.65(7)	
O(1)−Mn(1)−O(2)^a	103.81(6)	103.47(7)	106.92(6)	O(6)^b-Mn(2)−O(8)^b	91.84(7)	86.74(7)	
O(2)−Mn(1)−O(2)^a	180.00	180.00	180.00	O(7)^b−Mn(2)−O(8)^b	86.34(7)	86.63(7)	
O(2)−Mn(1)−O(4)	87.85(7)	87.23(7)	89.97(6)	O(7)−Mn(2)−O(8)	86.34(7)	86.63(7)	
O(1)^a−Mn(1)−O(2)	103.81(6)	103.47(7)	106.92(6)	O(6)^b−Mn(2)−O(7)	104.52(7)	105.35(7)	
Ni(1)−O(1)−Mn(1)	97.74(7)	97.34(8)	98.31(7)	Ni(2)−O(6)−Mn(2)	95.52(7)	95.83(8)	
Ni(1)−O(2)−Mn(1)	97.29(7)	96.58(8)	98.70(7)	Ni(2)−O(7)−Mn(2)	98.36(8)	95.87(7)	

^{a}Symmetry element $2-x, -y, -z$ in **1A**, $-x, -3-y, -3-z$ in **2A**, and $2-x, 1-y, 2-z$ in **3A**. ^{b}Symmetry element $2-x, 1-y, 1-z$ in **1B** and $-x, -4-y, -4-z$ in **2B**.

the simulations. In the model, the crystallographic equivalence of the two Ni^{II} ions in the trinuclear unit was considered by assigning one single g value for that ion. Additionally, a single set of magnetic parameters was deduced for each of the studied compounds, regardless of the presence of two nonequivalent Ni_2Mn trinuclear molecules in the unit cell in **1** and **2**. Simulations were carried out including a zero-field splitting (D) value for the two Ni^{II} ions and considering that the exchange coupling between these two terminal ions was zero (J_{Ni-Ni} = 0 cm^{-1}). Moreover, a term accounting for intermolecular interactions (zJ') was also included. The best agreement between experimental and simulated curves was obtained with the following sets of parameters: gNi = 2.10, g_{Mn} = 2.00, D_{Ni} = 4.0 cm^{-1}, J_{Ni-Mn} = 1.38 cm^{-1}, and zJ' = −0.06 cm^{-1} for complex **1**; g_{Ni} = 2.10, g_{Mn} = 2.00, D_{Ni} = 4.0 cm^{-1}, J_{Ni-Mn} = 0.50 cm^{-1}, and zJ' = −0.06 cm^{-1} for complex **2**; g_{Ni} = 2.10, g_{Mn} = 2.00, D_{Ni} = 4.0 cm^{-1}, J_{Ni-Mn} = −0.24 cm^{-1}, and zJ' = −0.03 cm^{-1} for complex **3**. The D parameter was fixed in the simulations and assumed to have the same value for complexes **1**−**3** in order to avoid overparametrization. Moreover, the intermolecular magnetic coupling (zJ') and the D parameter are very closely related and their independent contributions cannot be easily accounted for. This result indicates that, in addition to the intramolecular coupling, the zero-field splitting and the intermolecular coupling are present but their correct evaluation is not possible, given their close relation, as was also found in various Ni(II) complexes.[2c,d]

dx.doi.org/10.1021/ic501425x | Inorg. Chem. 2014, 53, 9296−9305

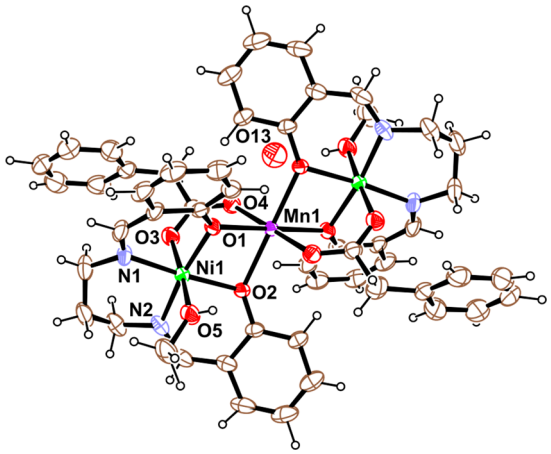

Figure 2. ORTEP-3 view of the centrosymmetric trinuclear structure of **2A** with ellipsoids at the 30% probability level. There are two trimers with equivalent structures; only one is shown.

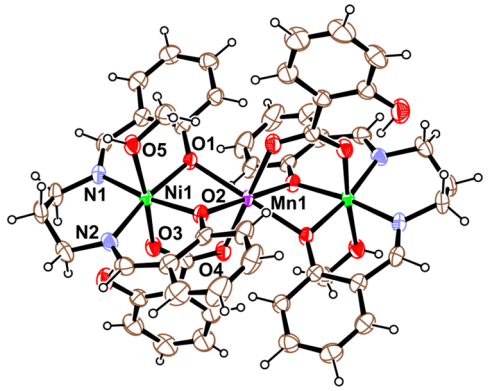

Figure 3. ORTEP-3 view of the centrosymmetric trinuclear structure of **3A** with ellipsoids at the 30% probability level.

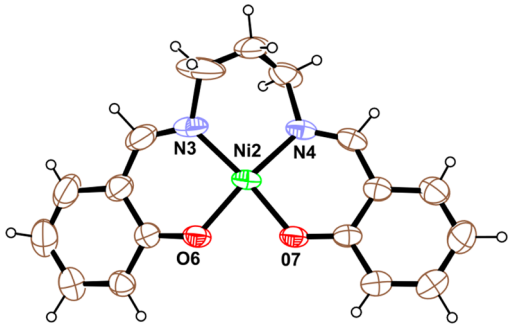

Figure 4. ORTEP-3 view of **3B** with ellipsoids at the 30% probability level.

Discussion. In all complexes, Ni^{II} and Mn^{II} centers are linked through two monodentate oxygen atoms coming from the deprotonation of two phenol groups that belong to the same ligand L and simultaneously by a bidentate carboxylate group coordinated to the metal ions in a *syn-syn* mode. One of the parameters that has been observed to have a crucial effect on the magnetic coupling between ions is the M−O−M′ angle from the monodentate bridge, M and M′ being the same or different metallic ions. There seems to be a critical value of the angle above which the superexchange is antiferromagnetic and below which the interaction becomes ferromagnetic, and this is called the critical angle. Actually, the critical angle has been very

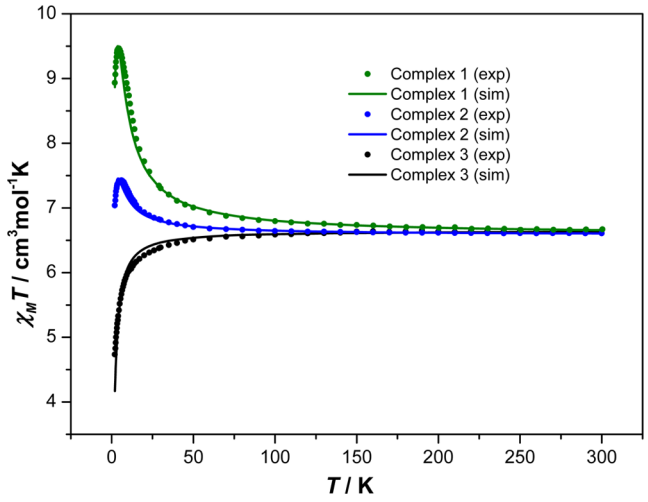

Figure 5. Thermal dependence of the $\chi_M T$ values for complexes **1**−**3**. Symbols represent experimental data, while solid lines represent the simulations obtained from the parameters indicated in the main text.

accurately determined for μ_2-phenoxido-bridged Cu^{II} homonuclear compounds.[1a] However, there is still a lack of empirical information on the effect of this angle in coordination complexes other than those based on Cu^{II} ions, not to mention in the heteropolynuclear compounds. Nevertheless, there is the possibility that other metallic ions or the combination of different metallic ions with a similar M−O−M′ skeleton might *push* this angle to higher values in order to obtain ferromagnetic complexes with a larger variety of geometries. In fact, and keeping this in mind, we decided to compare the value of this angle for the very limited amount of μ_2-phenoxido-bridged Ni_2Mn compounds reported so far that might also present *syn-syn* carboxylate bridges to fulfill the coordination sphere of their paramagnetic ions; hence, they are easily comparable in all terms. *syn-syn* carboxylate bridges have often been observed to lead to antiferromagnetic interactions in homonuclear complexes.[33] However, the heterometallic nature of the complexes studied in this work can effectively weaken such antiferromagnetic exchange, as explained later, and thus it has not been considered for simplicity. Table 3 shows the main structural features of those compounds, including those reported in this work, ordered by decreasing value of the magnetic exchange constant obtained from either the fit or the simulation of the experimental data.

As can be seen from Table 3, the number of μ_2-phenoxido bridges between the Ni^{II} and Mn^{II} centers is directly correlated with the Ni−O−Mn angle, 86.38° being the lowest in the case where there are three bridges and 102.31° the largest when only one phenoxide is bridging the magnetic ions. Our complexes, in which the two ions are linked by two monodentate phenoxide bridges, show very similar angles with an average value of 97.24° for **1**, 96.43° for **2**, and 98.51° for **3**, these three values being between those previously mentioned. Concerning the value of the magnetic exchange constant (J_{Ni-Mn}), this seems to follow a similar trend, by which low values of the angle induce ferromagnetic coupling while the largest values lead to antiferromagnetic exchange. A linear fit showing a possible dependence of the magnetic exchange constant J_{Ni-Mn} on the Ni−O−Mn angle is shown in Figure 6. The fit with an adjusted R^2 value of 0.88 indicates that the critical angle for μ_2-phenoxido-bridged Ni^{II}−Mn^{II} complexes could be around 99°.

dx.doi.org/10.1021/ic501425x | *Inorg. Chem.* 2014, 53, 9296−9305

Table 3. Selected Structural Parameters of μ_2-Phenoxido-Bridged Ni_2Mn Complexes, Ordered by Decreasing Value of the Magnetic Exchange Constant

compound	J_{Ni-Mn}(exptl)/cm^{-1}	J_{Ni-Mn}(calcd)/cm^{-1}	no. of μ_2-phenoxido bridges	Ni−O−Mn angle/deg	ref
$[Mn^{II}(Ni^{II}L)_2]\cdot 2CH_3OH$	+9.30	+8.3 (−0.3)	3	86.38	8
complex **1**[a]					
av	+1.38	+1.0	2	97.24	this work
1		+1.2 (−0.3)	2	96.89	
2		+0.8 (−0.3)	2	97.61	
complex **2**[a]					
av	+0.50	+0.25	2	96.43	this work
1		−0.4 (−0.3)	2	95.87	
2		+0.9 (−0.3)	2	96.99	
complex **3**	−0.24	−1.4 (−0.2)	2	98.51	this work
$[Mn^{II}(Ni^{II}L)_2(OAc)_4(H_2O)_2]$	−0.30	−3.4 (−0.1)	1	102.31	7

[a]Two nonequivalent molecules in the unit cell.

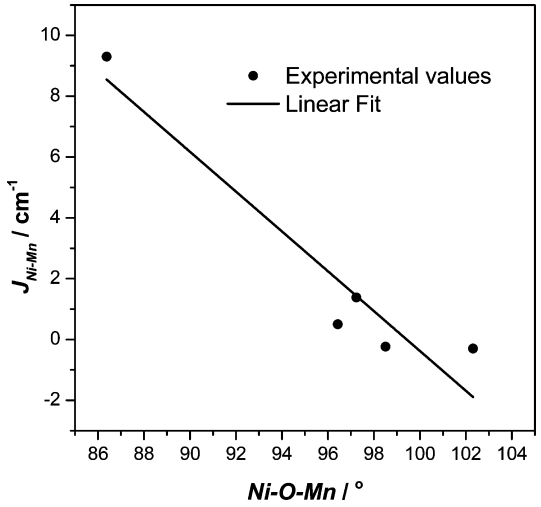

Figure 6. Variation of the magnetic coupling (J_{Ni-Mn}) in trinuclear Ni_2Mn double-phenoxido-bridged complexes with the average Ni−O−Mn bond angle. Data are extracted from complexes **1**−**3** of the present work and from complex **1** of ref 8 and complex **2** of ref 7.

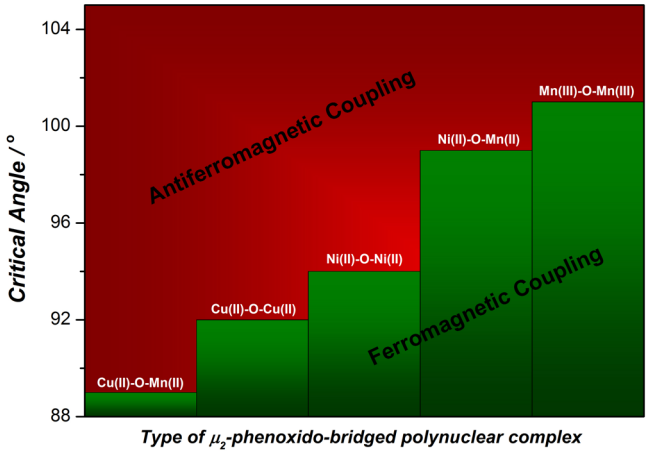

Figure 7. Critical angles for five different families of μ_2-phenoxido-bridged M−M′ polynuclear compounds. For homometallic polynuclear complexes, these values have been extracted from refs 1a, 3d, e, and 33. The values of the critical angles associated with heterometallic polynuclear complexes have been tentatively assigned on the basis of correlations established in this work and in ref 6e.

However, complex **2** shows the lowest Ni−O−Mn angle among the complexes reported in this work and thus the strongest ferromagnetic exchange is expected for complex **2** in comparison to complexes **1** and **3**. Nevertheless, complex **2** shows an intermediate J_{Ni-Mn} value, lower than that of complex **1**. The crystal structure of complex **2** shows two nonequivalent molecules in the structure, one of which presents a coordination number of 5 for its two Ni^{II} ions, as opposed to all other Ni^{II} centers in complexes **1**−**3**, where they are 6-coordinated. This fact strongly affects the Ni^{II}−Mn^{II} magnetic exchange interaction in this complex, and it is the reason for such disagreement in the magnetostructural correlation, as will be shown later by means of theoretical calculations. The critical angles for five different families of μ_2-phenoxido-bridged M−M′ polynuclear compounds have been depicted in Figure 7, where the critical angle is defined as the M−O−M′ angle formed by the monodentate phenoxido-based bridging ligand. While for homometallic polynuclear complexes of Cu^{II}, Ni^{II}, or Mn^{III} ions these values have been extracted or assigned from the results reported in the literature by other authors,[1a,3d,e,34] the values of the critical angles associated with heterometallic polynuclear complexes such as Ni^{II}−Mn^{II} and Cu^{II}−Mn^{II} systems have been tentatively assigned on the basis of correlations established with Schiff base trinuclear complexes studied by us in this work and in ref 6e, respectively. Apparently, among the five different families of polynuclear compounds compared, the heterometallic family based on Cu^{II}−Mn^{II} ions shows the lowest critical angle of all, restricting the range of angles that lead to ferromagnetic exchange in comparison to more established homometallic compounds made of Cu^{II}, Ni^{II}, or Mn^{III} ions. On the other hand, the family of heterometallic complexes based on Ni^{II}−Mn^{II} ions could represent an increase of this value up to ca. 99°, comparable to the value reported for μ_2-phenoxido-bridged Mn^{III}-based homometallic complexes and significantly higher than that reported for analogous Ni^{II}-based homometallic complexes. Still, Mn(III)-based homometallic complexes show the highest critical angle at 101°,[3d,e] thus remaining as the family of μ_2-phenoxido-bridged polynuclear complexes with the largest range of angles available for ferromagnetic exchange. Despite this, similar heterometallic compounds based on Mn^{III} ions have been rarely studied from this point of view and definitely deserve more attention due to the potential they hold.

Theoretical Results. The calculated exchange coupling constants (see Computational Details) of the three synthesized Ni_2Mn complexes (**1**−**3**) together with those of two systems previously reported are collected in Table 3 and depicted in

dx.doi.org/10.1021/ic501425x | Inorg. Chem. 2014, 53, 9296−9305

Figure 8.[7,8] As shown in Figure 8, there is a clear magneto-structural correlation between the Ni−O−Mn angle and the J_{Ni-Mn} values, in agreement with what was observed experimentally (Figure 6). The coordination number of the Ni^{II} cations is 6, with the exception of one of the molecules of complex **2** (black circle in Figure 8 and antiferromagnetic

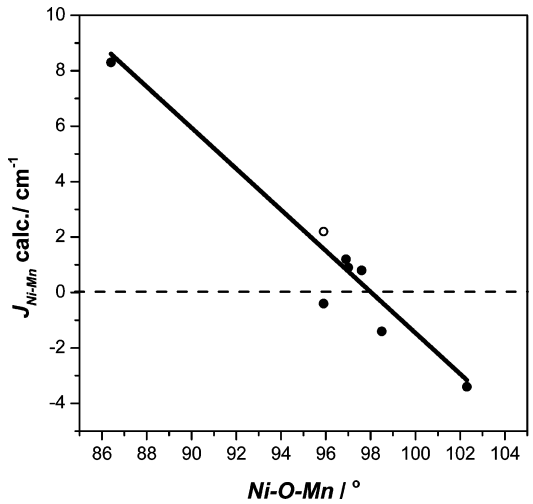

Figure 8. Dependence between the calculated J_{Ni-Mn} values and the average Ni−O−Mn angle of the μ_2-phenoxido bridging ligands. For molecule 1 of complex **2**, with a Ni−O−Mn angle of 95.87°, an antiferromagnetic coupling with J_{Ni-Mn} = −0.4 cm^{-1} was found experimentally (black circle), since Ni^{II} centers are five-coordinated. A J_{Ni-Mn} value of +2.2 cm^{-1} is calculated (white circle) by adding a methanol molecule to give the same coordination number as for the other systems.

coupling of −0.4 cm^{-1} in Table 3). However, the inclusion of a methanol molecule in this structure to reach the coordination number of 6 present in all the other cases results in a ferromagnetic coupling of +2.2 cm^{-1} (white circle in Figure 8), improving the magnetostructural correlation expressed by a linear regression with an adjusted R^2 value of 0.97. The calculation of next-nearest-neighbor J_{Ni-Ni} constants shows that all cases correspond to weak antiferromagnetic couplings. Futhermore, these J_{Ni-Ni} values become slightly less antiferromagnetic when the Ni−O−Mn angle is increased, just the opposite behavior of the J_{Ni-Mn} couplings.

As pointed out in Figure 7, the interaction between Ni^{II} and Mn^{II} centers needs a relatively large Ni−O−Mn critical angle to become antiferromagnetic. In order to justify this fact, we can apply a simple rule based on the Kahn−Briat model.[35−37] By considering the number and symmetry of interactions of pairs of magnetic orbitals for the Ni^{II}−Mn^{II} systems, we can expect respectively two antiferromagnetic and eight ferromagnetic contributions. For instance, only one of the five d orbitals of Mn^{II} will have the right symmetry to give an antiferromagnetic contribution in its interaction with each one of the two orbitals bearing the unpaired electrons of the Ni^{II} center. Due to the relatively high number of ferromagnetic contributions, the Ni^{II}−Mn^{II} systems have a large tendency to show ferromagnetic coupling, and only large Ni−O−Mn angles (above 98°) can induce antiferromagnetism.

The calculated spin density distribution for the ground state of complex **1** showing ferromagnetic coupling between Ni^{II} and Mn^{II} centers (see Table 3) is represented in Figure 9. As expected, due to the d^5 electronic configuration of the Mn^{II}

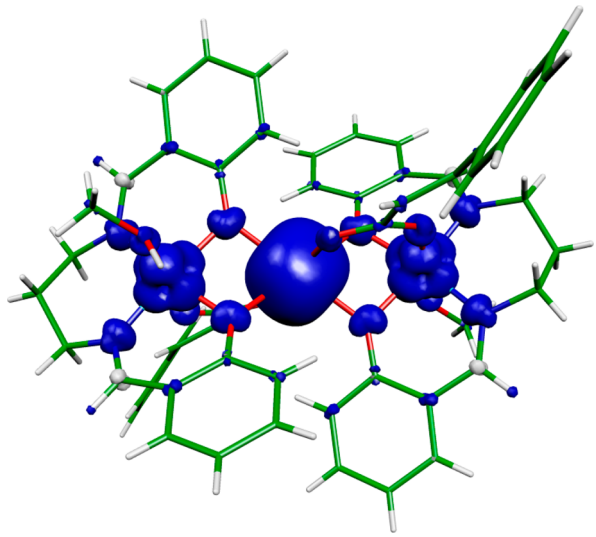

Figure 9. Spin density distribution for complex **1** corresponding to the S = 9/2 ground state. The isodensity surface represented corresponds to a value of 0.005 e/bohr^3 (positive and negative values are represented as blue and white surfaces, respectively).

cation, the spin distribution is almost spherical, while in the Ni^{II} centers it is the square of the sum of the d_{z^2} and $d_{x^2-y^2}$ magnetic orbitals. Due to the presence of unpaired electrons in all of the antibonding metal−ligand orbitals (those of t_{2g} symmetry assuming O_h symmetry), there is a predominance of the spin delocalization due to the strong mixing of metal−ligand orbitals.[38,39] This fact results in all the atoms coordinated to the metals having the same sign of spin population. Small white lobes in some of the carbon atoms of the terminal ligands indicate that the spin polarization mechanism prevails in the atoms of the second coordination sphere.

CONCLUSIONS

Three new Ni^{II}−Mn^{II} complexes derived from a salen type Schiff base ligand along with various *syn-syn* bridging carboxylate coligands, viz. cinnamate, phenylacetate, and salicylate, have been synthesized and characterized in order to determine the crossover angle experimentally. All three have similar trinuclear structures comprised of a central octahedral Mn^{II} and two terminal octahedral or square-pyramidal Ni^{II} atoms having slight variations in Ni−O−Mn angles (96.43−98.51°). A linear dependence was found in these Ni^{II}−Mn^{II} diphenoxido-bridged complexes between the J_{Ni-Mn} value and the Ni−O−Mn angle of the monodentate phenoxido bridges, from which a high value of the crossover angle from ferro- to antiferromagnetic exchange could be assigned. This value corresponds approximately to 98° and apparently indicates that the family of Ni^{II}−Mn^{II} complexes is that which supports ferromagnetic interactions for a higher angle among the various known MM′ diphenoxido-bridged complexes, with the exception of the $Mn^{III}Mn^{III}$ compounds. Theoretical calculations also indicate that an incomplete octahedral coordination sphere for these ions can significantly alter this correlation, and thus it is only valid for six-coordinated species.

ASSOCIATED CONTENT

Supporting Information

CIF files giving crystallographic data for **1**−**3**. This material is available free of charge via the Internet at http://pubs.acs.org.

dx.doi.org/10.1021/ic501425x | *Inorg. Chem.* 2014, 53, 9296−9305

AUTHOR INFORMATION

Corresponding Authors

*E-mail for A.F.: albert.figuerola@qi.ub.edu.
*E-mail for A.G.: ghosh_59@yahoo.com.

Notes

The authors declare no competing financial interest.

ACKNOWLEDGMENTS

We thank the DST-FIST of India funded Single Crystal Diffractometer Facility at the Department of Chemistry, University of Calcutta, Kolkata, India. The authors thank the Department of Science and Technology (DST), New Delhi, India, for financial support (SR/S1/IC/0034/2012). P.S. is grateful to the UGC for a research fellowship (UGC/52/Jr. Fellow (Enhancement) dated 17.01.2013). A.F. acknowledges financial support from the Spanish MINECO through CTQ2012-32247 and for a Ramón y Cajal Fellowship (RYC-2010-05821). J.J. and E.R. thank the Spanish Ministerio de Economia y Competitividad (CTQ2011-23862-C02-01) and the regional Generalitat de Catalunya authority (2009SGR-1459). The authors gratefully acknowledge the computer resources, technical expertise, and assistance provided by the CESCA.

REFERENCES

(1) (a) Yazigia, D. V.; Aravenab, D.; Spodineb, E.; Ruiz, E.; Alvarez, S. *Coord. Chem. Rev.* **2010**, *254*, 2086−2095 and references therein. (b) Biswas, C.; Drew, M. G. B.; Ruiz, E.; Estrader, M.; Diaz, C.; Ghosh, A. *Dalton Trans.* **2010**, *39*, 7474−7484. (c) Ding, C.; Gao, C.; Ng, S.; Wang, B.; Xie, Y. *Chem. Eur. J.* **2013**, *19*, 9961−9972. (d) Ray, A.; Mitra, S.; Khalaji, A. D.; Atmani, C.; Cosquer, N.; Triki, S.; Juan, J. M. C.; Serra, S. C.; Gómez-García, C. J.; Butcher, R. J.; Garribba, E.; Xuh, D. *Inorg. Chim. Acta* **2010**, *363*, 3580−3588.

(2) (a) Biswas, R.; Kar, P.; Song, Y.; Ghosh, A. *Dalton Trans.* **2011**, *40*, 5324−5331. (b) Nanda, K. K.; Das, R.; Thompson, L. K.; Venkatsubramanian, K.; Nag, K. *Inorg. Chem.* **1994**, *33*, 1188−1193. (c) Mukherjee, P.; Drew, M. G. B.; Gomez-García, C. J.; Ghosh, A. *Inorg. Chem.* **2009**, *48*, 5848−5860. (d) Mukherjee, P.; Drew, M. G. B.; Tangoulis, V.; Estrader, M.; Diaz, C.; Ghosh, A. *Polyhedron* **2009**, *28*, 2989−2996.

(3) (a) Chumillas, M. V.; Tanase, S.; Mutikainen, I.; Turpeinen, U.; de Jongh, L. J.; Reedijk, J. *Inorg. Chem.* **2008**, *47*, 5919−5929. (b) Watkinson, M.; Fondo, M.; Bermejo, M. R.; Sousa, A.; McAuliffe, C. A.; Pritchard, R. G.; Jaiboon, N.; Aurangzeb, N.; Naeem, M. *J. Chem. Soc., Dalton Trans.* **1999**, 31−42. (c) Sailaja, S.; Reddy, K. R.; Rajasekharan, M. V.; Hureau, C.; Riviere, E.; Cano, J.; Girerd, J.-J. *Inorg. Chem.* **2003**, *42*, 180−186. (d) Lu, Z.; Yuan, M.; Pan, F.; Gao, S.; Zhang, D.; Zhu, D. *Inorg. Chem.* **2006**, *45*, 3538−3548. (e) Bhargavi, G.; Rajasekharan, M. V.; Costes, J.-P.; Tuchagues, J.-P. *Polyhedron* **2009**, *28*, 1253−1260. (f) Kar, P.; Guha, P. M.; Drew, M. G. B.; Ishida, T.; Ghosh, A. *Eur. J. Inorg. Chem.* **2011**, 2075−2085. (g) Kar, P.; Biswas, R.; Drew, M. G. B.; Ida, Y.; Ishida, T.; Ghosh, A. *Dalton Trans.* **2011**, *40*, 3295−3304. (h) Kar, P.; Haldar, R.; Gómez-García, C. J.; Ghosh, A. *Inorg. Chem.* **2012**, *51*, 4265−4273. (i) Seth, P.; Drew, M. G. B.; Ghosh, A. *J. Mol. Catal. A: Chem.* **2012**, *365*, 154−161.

(4) (a) Ruiz, E.; Alemany, P.; Alvarez, S.; Cano, J. *Inorg. Chem.* **1997**, *36*, 3683−3688. (b) Burkhardt, A.; Spielberg, E. T.; Simon, S.; Gçrls, H.; Buchholz, A.; Plass, W. *Chem. Eur. J.* **2009**, *15*, 1261−1271.

(5) (a) Biswas, S.; Ghosh, A. *Polyhedron* **2013**, *65*, 322−331. (b) Biswas, S.; Diaz, C.; Ghosh, A. *Polyhedron* **2013**, *51*, 96−101. (c) Tao, R.-J.; Mei, C.-Z.; Zang, S.-Q.; Wang, Q.-L.; Niu, J.-Y.; Liao, D.-Z. *Inorg. Chim. Acta* **2004**, *357*, 1985−1990. (d) Journaux, Y.; Khan, O.; Badarau, I. M.; Galy, J.; Jaud, J.; Bencini, A.; Gatteschi, D. *J. Am. Chem. Soc.* **1985**, *107*, 6305−6312.

(6) (a) Biswas, S.; Naiya, S.; Gómez-García, C. J.; Ghosh, A. *Dalton Trans.* **2012**, *41*, 462−473. (b) Mei, C. Z.; Tao, R.-J.; Wang, Q.-L. *Acta Chim. Sin.* **2007**, *65*, 1129−1134. (c) Brychcy, K.; Jens, K.-J.; Tilset, M.; Behrens, U. *Chem. Ber.* **1994**, *127*, 991−995. (d) Öz, S.; Kurtaran, R.; Arici, C.; Ergun, Ü.; Kaya, F. N. D.; Emregül, K. C.; Atakol, O.; Ülkü, D. *J. Therm. Anal. Calorim.* **2010**, *99*, 363−368. (e) Seth, P.; Ghosh, S.; Figuerola, A.; Ghosh, A. *Dalton Trans.* **2014**, *43*, 990−998.

(7) Sharma, A. K.; Lloret, F.; Mukherjee, R. *Inorg. Chem.* **2007**, *46*, 5128−5130.

(8) Kobayashi, T.; Yamaguchi, T.; Ohta, H.; Sunatsuki, Y.; Kojima, M.; Re, N.; Nonoyama, M.; Matsumoto, N. *Chem. Commun.* **2006**, 1950−1952.

(9) (a) Sari, M.; Atakol, O.; Svoboda, I. *Anal. Sci.: X-Ray Struct. Anal. Online* **2005**, *21*, x205−x206. (b) Ercan, F.; Atakol, O. *Acta Crystallogr., Sect. C: Cryst. Struct. Commun.* **1998**, *54*, 1268−1270. (c) Ercan, F.; Atakol, O.; Arici, C.; Svoboda, I.; Fuess, H. *Acta Crystallogr., Sect. C: Cryst. Struct. Commun.* **2002**, *58*, m193−m196. (d) Atakol, O.; Nazir, H.; Durmus, Z.; Svoboda, I.; Fuess, H. *Anal. Sci.* **2002**, *18*, 493. (e) Chen, H.; Ma, C. B.; Yuan, D. Q.; Hu, M.-Q.; Wen, H.-M.; Liu, Q.-T.; Chen, C.-N. *Inorg. Chem.* **2011**, *50*, 10342−10352.

(10) (a) Biswas, S.; Naiya, S.; Drew, M. G. B.; Estarellas, C.; Frontera, A.; Ghosh, A. *Inorg. Chim. Acta* **2011**, *366*, 219−226. (b) Das, L. K.; Park, S.-W.; Choc, S. J.; Ghosh, A. *Dalton Trans.* **2012**, *41*, 11009−11017. (c) Ghosh, A. K.; Bauzá, A.; Bertolasi, V.; Frontera, A.; Ray, D. *Polyhedron* **2013**, *53*, 32−39.

(11) Reglinski, J.; Morris, S.; Stevenson, D. E. *Polyhedron* **2002**, *21*, 2167−2174.

(12) Drew, M. G. B.; Prasad, R. N.; Sharma, R. P. *Acta Crystallogr., Sect. C: Cryst. Struct. Commun.* **1985**, *41*, 1755−1758.

(13) Ruiz, E.; Alemany, P.; Alvarez, S.; Cano, J. *J. Am. Chem. Soc.* **1997**, *119*, 1297−1303.

(14) Ruiz, E. *Struct. Bonding (Berlin)* **2004**, *113*, 71.

(15) Ruiz, E.; Rodríguez-Fortea, A.; Cano, J.; Alvarez, S.; Alemany, P. *J. Comput. Chem.* **2003**, *24*, 982−989.

(16) Ruiz, E.; Alvarez, S.; Cano, J.; Polo, V. *J. Chem. Phys.* **2005**, *123*, 164110.

(17) Ruiz, E.; Fortea, A. R.; Tercero, J.; Cauchy, T.; Massobrio, C. *J. Chem. Phys.* **2005**, *123*, 074102.

(18) Becke, A. D. *J. Chem. Phys.* **1993**, *98*, 5648−5652.

(19) Frisch, M. J.; Trucks, G. W.; Schlegel, H. B.; Scuseria, G. E.; Robb, M. A.; Cheeseman, J. R.; Scalmani, G.; Barone, V.; Mennucci, B.; Petersson, G. A.; Nakatsuji, H.; Caricato, M.; Li, X.; Hratchian, H. P.; Izmaylov, A. F.; Bloino, I. J.; Zheng, G.; Sonnenberg, J. L.; Hada, M.; Ehara, M.; Toyota, K.; Fukuda, R.; Hasegawa, J.; Ishida, M.; Nakajima, T.; Honda, Y.; Kitao, O.; Nakai, H.; Vreven, T.; Montgomery, J. A., Jr.; Peralta, J. E.; Ogliaro, F.; Bearpark. M.; Heyd, J. J.; Brothers, E.; Kudin, K. N.; Staroverov, V. N.; Kobayashi, R.; Normand, J.; Raghavachari, K.; Rendell, A.; Burant, J. C.; Iyengar, S. S.; Tomasi, J.; Cossi, M.; Rega, N.; Millam, J. M.; Klene, M.; Knox, J. E.; Cross, J. B.; Bakken, V.; Adamo, C.; Jaramillo, J.; Gomperts, R.; Stratmann, R. E.; Yazyev, O.; Austin, A. J.; Cammi, C.; Pomelli, J. W.; Ochterski, R.; Martin, R. L.; Morokuma, K.; Zakrzewski, V. G.; Voth, G. A.; Salvador, P.; Dannenberg, J. J.; Dapprich, S.; Daniels, A. D.; Farkas, O.; Foresman, J. B.; Ortiz, J. V.; Cioslowski, J.; Fox, D. J. *Gaussian 09 (Revision D01)*; Gaussian, Inc., Wallingford, CT, 2009.

(20) *Jaguar 7.0*; Schrödinger, LLC, New York, 2007.

(21) Vacek, G.; Perry, J. K.; Langlois, J.-M. *Chem. Phys. Lett.* **1999**, *310*, 189−194.

(22) Schaefer, A.; Huber, C.; Ahlrichs, R. *J. Chem. Phys.* **1994**, *100*, 5829−5835.

(23) *SAINT, version 6.02, and SADABS, version 2.03*; Bruker AXS, Inc., Madison, WI, 2002.

(24) Sheldrick, G. M. *SHELXS-97, program for solution of crystal structures*; University of Göttingen, Göttingen, Germany, 1997.

(25) Sheldrick, G. M. *SHELXL-97, program for refinement of crystal structures*; University of Göttingen, Göttingen, Germany, 1997.

(26) Spek, A. L. *Acta Crystallogr., Sect. A: Found. Crystallogr.* **1990**, *46*, C34.

(27) Farrugia, L. J. *J. Appl. Crystallogr.* **1997**, *30*, 565.

(28) Farrugia, L. J. *J. Appl. Crystallogr.* **1999**, *32*, 837.

(29) Addison, A. W.; Rao, T. N.; Reedjik, J.; Rijn, J. V.; Verschoor, C. G. *J. Chem. Soc., Dalton Trans.* **1984**, 1349−1356.
(30) (a) Seth, P.; Das, L. K.; Drew, M. G. B.; Ghosh, A. *Eur. J. Inorg. Chem.* **2012**, 2232−2242. (b) Das, L. K.; Drew, M. G. B.; Ghosh, A. *Inorg. Chim. Acta* **2013**, *394*, 247−254. (c) Das, L. K.; Biswas, A.; Gómez-García, C. J.; Drew, M. G. B.; Ghosh, A. *Inorg. Chem.* **2014**, *53*, 434−445.
(31) Yang, L.; Powell, D. R.; Houser, R. P. *Dalton Trans.* **2007**, 955−964.
(32) (a) Almenar, J. J. B.; Juan, J. M. C.; Coronado, E.; Tsukerblat, B. S. *J. Comput. Chem.* **2001**, *22*, 985−991. (b) Almenar, J. J. B.; Juan, J. M. C.; Coronado, E.; Tsukerblat, B. S. *Inorg. Chem.* **1999**, *38*, 6081−6088.
(33) Ghoshal, D.; Maji, T. K.; Mostafa, G.; Sain, S.; Lu, T.-H.; Ribas, J.; Zangrando, E.; Chaudhuri, N. R. *Dalton Trans.* **2004**, 1687−1695.
(34) (a) Bu, X.-H.; Du, M.; Zhang, L.; Liao, D.-Z.; Tang, J.-K.; Zhang, R.-H.; Shionoya, M. *J. Chem. Soc., Dalton Trans.* **2001**, 593−598. (b) Biswas, R.; Giri, S.; Saha, S. K.; Ghosh, A. *Eur. J. Inorg. Chem.* **2012**, 2916−2927.
(35) Kahn, O.; Briat, B. *J. Chem. Soc., Faraday Trans. 2* **1976**, *72*, 268−281.
(36) Kahn, O.; Briat, B. *J. Chem. Soc., Faraday Trans. 2* **1976**, *72*, 1441−1446.
(37) Kahn, O. *Molecular Magnetism*; VCH: New York, 1993.
(38) Ruiz, E.; Cirera, J.; Alvarez, S. *Coord. Chem. Rev.* **2005**, *249*, 2649−2660.
(39) Cano, J.; Ruiz, E.; Alvarez, S.; Verdaguer, M. *Comments Inorg. Chem.* **1998**, *20*, 27−56.